NASA Technical Memorandum 81456

CALCULATION OF RESIDUAL PRINCIPAL STRESSES IN CVD BORON ON CARBON FILAMENTS

Donald R. Behrendt
Lewis Research Center
Cleveland, Ohio

Prepared for the
Fourth Annual Conference on Composites and Advanced Materials
sponsored by the American Ceramic Society
Cocoa Beach, Florida, January 21-24, 1980

CALCULATION OF RESIDUAL PRINCIPAL STRESSES IN CVD BORON ON CARBON FILAMENTS

by Donald R. Behrendt

National Aeronautics and Space Administration
Lewis Research Center
Cleveland, Ohio 44135

ABSTRACT

A three-dimensional finite element model of the chemical vapor deposition (CVD) of boron on a carbon substrate (B/C) is developed. The model includes an expansion of the boron after deposition due to atomic rearrangement and includes creep of the boron and carbon. Curves are presented to show how the principal residual stresses and the filament elongation vary as the parameters defining deposition strain and creep are varied. The calculated results are compared with experimental axial residual stress and elongation measurements made on B/C filaments. This comparison requires that for good agreement between calculated and experimental results, the deposited boron must continue to expand after deposition, and that the build-up of residual stresses is limited by significant boron and carbon creep rates.

E-386

INTRODUCTION

Boron filaments made by the chemical vapor deposition (CVD) of boron onto a tungsten or carbon substrate exhibit high moduli and strengths; however, a detailed understanding of the elongation of the filament during deposition and the large residual stresses in the resulting filament is yet needed. For boron deposited on a carbon substrate (B/C), this elongation is as much as 5 percent (Ref. 1). Measurements of the axial residual stresses in 102 μm (4.0 mil) diameter B/C filament show these stresses to be large, 790 MPa (115 ksi) compressive stress near the surface and 290 MPa (42 ksi) tensile stress near the carbon core (Ref. 2).

Witucki (Ref. 3) estimated the residual stresses by assuming that the boron is deposited in a stressed state and that the boron behaved elastically. His calculated axial residual stress distribution, although agreeing with experimental values at the surface, increased rapidly for decreasing radial

location inside the filament to values much larger than are observed experimentally. Mehalso (Ref. 1) suggested that the residual stresses and the elongation were produced by an expansion of the boron after deposition due to atomic rearrangement. Eason (Ref. 4) has measured the elongation during the chemical vapor deposition of boron on tungsten and boron on carbon. Eason, using a one-dimensional model in which he assumes, as did Mehalso, that the boron continues to expand after deposition and that the residual stresses are limited to a given maximum value, calculated the filament elongation during boron deposition. Although he obtained good agreement between his calculated and measured elongation results, his model did not give good agreement with the measured axial residual stresses. Because his model was one-dimensional, he was not able to calculate the radial and circumferential stresses.

The objective of the work reported here was to develop a three-dimensional model of chemical vapor deposition of boron and to use this to calculate residual stresses and elongation of the filament during deposition. Because the model developed was three-dimensional, the principal stresses in the radial, circumferential, and axial directions could all be calculated. In this model, the boron was allowed to expand after deposition as suggested by Mehalso and used by Eason in his model. In addition, the boron was allowed to creep according to a stress-dependent creep law. These two additions in this model (the use of three dimensions and the stress-dependent creep) produce calculated results for the residual stresses and filament elongation in excellent agreement with experimental measurements.

DEPOSITION MODEL

It is assumed in this model that the filament is always axisymmetric. The elements in the finite element analysis used were taken to be cylindrical shells as shown in Figure 1. Here, r_c is the core (substrate) radius, and r_i is the outer radius of the i^{th} shell or element. The nodes of the i^{th} element are then located at r_{i-1} and r_i. Because of this symmetry, it is necessary to determine the nodal displacements in the radial and axial directions. The nodal displacements, u_i, in the radial direction are obtained by the method of finite element analysis. The nodal displacements, w_i, in the axial direction are the same for all nodes and are obtained from the condition of equilibrium that the net force in the axial direction on a face perpendicular to this direction is zero. From these nodal displacements, the principal

strains, ε_r, ε_θ, and ε_z in the radial, circumferential, and axial directions, respectively, can be calculated for each element. From these strains, the principal stresses σ_r, σ_θ, and σ_z can be calculated for each element.

In this model, it is assumed that the boron continues to expand after deposition. In the actual filament, such an expansion could be produced by the diffusion of boron from the surface into the bulk. The force driving such diffusion is now known; however, one might conclude that it depends upon the chemical vapor deposition process itself. If a boron filament is annealed in an atmosphere containing oxygen, which removes boron from the surface, the filament contracts (Ref. 4); however, it neither contracts or elongates if annealed in an oxygen-free nitrogen atmosphere (Ref. 4) which does not remove boron from the surface. It is also observed that voids grow at the boron core interface when boron filaments are annealed in an atmosphere which removes boron from the surface, indicating that some of the boron has diffused from core-sheath interface to the surface and is not merely due to the removal of surface boron atoms. It appears that deposition of boron on the surface causes an inward diffusion of boron.

The expansion is assumed to depend on the time after deposition of the boron according to

$$\left.\begin{aligned} \varepsilon''_{or} &= \varepsilon_{or}(1 - e^{-\alpha t}) \\ \varepsilon''_{o\theta} &= \varepsilon_{o\theta}(1 - e^{-\alpha t}) \\ \varepsilon''_{oz} &= \varepsilon_{oz}(1 - e^{-\alpha t}) \end{aligned}\right\} \qquad (1)$$

where t is the time after deposition of the boron in the given element, α is a reciprocal time constant, ε_{or}, $\varepsilon_{o\theta}$, and ε_{oz} are the maximum plastic strains attained as αt goes to infinity, and the double prime indicates that these are plastic strains. For large α, the plastic strains for a given element approach their maximum values before very many additional elements are added. This approaches Witucki's model in which the boron is deposited in a strained condition. For small α, boron in the first deposited elements continues to expand even as the final elements are deposited.

Due to these plastic deposition strains, stresses start to increase in the elements causing creep to take place. In this model, the following stress-

dependent creep equations are used to calculate the creep strains for each element. Following Lin (Ref. 5), the effective creep rate $\dot{\varepsilon}^*$ is given by

$$\dot{\varepsilon}^* = B\sigma^{*n} \tag{2}$$

where B and n are constants and σ^*, the effective stress, is

$$\sigma^* = \frac{1}{\sqrt{2}}\left[(\sigma_r - \sigma_\theta)^2 + (\sigma_\theta - \sigma_z)^2 + (\sigma_z - \sigma_r)^2\right]^{1/2} \tag{3}$$

The principal creep strains can then be defined in terms of $\dot{\varepsilon}^*$ and σ^* as (Ref. 5)

$$\left.\begin{aligned} \varepsilon_r'' &= \frac{\dot{\varepsilon}^*}{\sigma^*}\left(\sigma_r - \frac{\sigma_\theta + \sigma_z}{2}\right)\Delta t \\ \varepsilon_\theta'' &= \frac{\dot{\varepsilon}^*}{\sigma^*}\left(\sigma_\theta - \frac{\sigma_r + \sigma_z}{2}\right)\Delta t \\ \varepsilon_z'' &= \frac{\dot{\varepsilon}^*}{\sigma^*}\left(\sigma_z - \frac{\sigma_r + \sigma_\theta}{2}\right)\Delta t \end{aligned}\right\} \tag{4}$$

where Δt is the time required to deposit the outermost element and is proportional to $r_i^2 - r_{i-1}^2$. Equations (4) give the principal creep strains for an element in terms of the principal stresses for that element.

RESULTS

In this section, the dependence of the calculated residual stresses and filament elongation on the parameters in the deposition strain equations (Eqs. (1)) and the creep strain equations (Eqs. (2)) are shown. In these calculations, the elastic constants used for the carbon core and boron sheath are shown in Table I.

In order to keep the next three figures simple, only the dependence of the axial component of the calculated residual stresses on the parameters in deposition strain and creep equations is shown.

In Figure 2, the effect of varying B in the creep equations (Eq. (2)) on the axial residual stress, σ_z, is shown. For zero creep ($B = 0.0$) the

axial component varies from -2.95 GPa (-428 ksi) near the surface to 6.67 GPa (967 ksi) near the core. As B is increased from zero, the amount of creep increases with a comparable reduction in the residual stresses as shown by the curves for B = 3, 6, 9, 15, and 200×10^{19}.

In Figure 3, the effect of varying α in the deposition strain equations (Eq. (1)) on the axial residual stress, σ_z, is shown. Note that changes in α produce large changes in the shape of the curves for σ_z. In particular, the minimum just inside the outer surface changes from a broad minimum for small α to a narrow minimum for large α. In the limit as α goes to infinity, this minimum disappears (not shown in the figure). As α goes to zero, the surface value for σ_z goes to zero.

In Figure 4, the effect of simultaneously varying the parameters $\varepsilon_{o\theta}$ and ε_{oz} (Eq. (1)) on the axial residual stress, σ_z, is shown. Here $\varepsilon_{or} = 0.0$, and $\varepsilon_{o\theta}$ is set equal to ε_{oz}. The effects of varying this parameter are small near the core but become larger near the surface making large changes in the minimum near the surface.

In Figure 5, the effect of varying B in the creep equations (Eq. (2)) on the elongation of the filament is shown. This shows the percent elongation versus radius of the filament during the filament growth. The largest value of B shows the largest reduction in elongation.

In Figure 6, the effect of varying α in the deposition strain equation (Eq. (1)) on the elongation during filament growth is shown. As α increases, the elongation for a given radius also increases except for the larger values of α in which the elongation decreases for increasing values of α for values of r near the largest values shown.

In Figure 7, the effects of simultaneously varying $\varepsilon_{o\theta}$ and ε_{oz} (Eq. (1)) on the elongation during filament growth is shown. Here increasing $\varepsilon_{o\theta}$ and ε_{oz} markedly increases the elongation.

Comparison with Experimental Results

The parameters $\varepsilon_{o\theta}$, ε_{oz}, α, B, and n were adjusted to calculate a σ_z versus r curve which closely matched the experimental curve for a 102 μm (4.0 mil) diameter B/C filament. This is shown in Figure 8 along with an experimental curve. The experimental curve was obtained by the method described in Ref. 2. Several points should be made regarding these parameters. The

minimum in the experimental curve for σ_z near the surface is reasonably reproduced in the calculated curve when values of α are near 0.3. Based on this model, this means that the boron is not merely deposited in a strained state but that it continues to expand after deposition. The deep minimum at the core-sheath interface in the experimental curve could not be duplicated in the calculated curves. This experimentally observed minimum is probably the result of the small amount of interdiffusion between the carbon core and the boron sheath which was not modeled in the calculation. The lower value for the core residual stress in the experimental curve may result from the low shear strength of the pyrolytic graphite coating applied to the carbon substrate to reduce core fracture during boron deposition. Also, this was not considered in this model.

In Figure 9, the calculated curves for all three components of the residual stresses, σ_r, σ_θ, and σ_z are shown using the same values for the parameters as for the calculated curve in Figure 8. A comparison of the calculated curves for σ_r and σ_θ with experiment cannot be made because of the lack of comparable experimental data. However, the boundary condition at the surface requires that σ_r goes to zero as it does in this figure.

In Figure 10, the calculated elongation results and the experimental elongation curves of Mehalso (Ref. 1) for B/C are shown. The values of parameters for the calculated curve are the same as in Figures 8 and 9. The experimental data are for deposition temperatures of 1200° C and 1300° C are shown. Near the final radius, the slope of the calculated curve is decreasing more rapidly with radius than are the experimental curves. However, the calculated total elongation agrees with the experimental value.

CONCLUSIONS

The overall good agreement between the calculated and experimental curves for both the axial residual stress and elongation curves leads to the following conclusions:

1. The minimum near the surface in the experimental curve for σ_z is reasonably reproduced in the calculated curve for values of α near 0.3. This means that chemical vapor deposited boron continues to expand for some time after deposition. Such an expansion could result from boron diffusing from the surface into the bulk filling vacancies or adding additional planes of atoms.

2. Boron at the temperature of deposition must creep substantially as indicated by the large value of B required in Equation (2).

SUMMARY

A three-dimensional model of the chemical vapor deposition of boron on a carbon substrate was developed in which an expansion of the deposited boron and subsequent creep of the boron were included. The method of finite element analysis was used to obtain values of residual stresses σ_r, σ_θ, and σ_z as a function of radial location, r, in the completed filament and the elongation of the filament as a function of its growth radius. A wide range of values for parameters in the deposition strain equations and creep equations were used. Comparison of the calculated results with experimental results for the axial residual stresses and elongation of B/C filaments indicate that the boron continues to expand for some time after deposition and that the boron creeps which limits the build-up of residual stresses.

REFERENCES

1. R. M. Mehalso, "Chemical Vapor Deposition of Boron on a Carbon Monofilament Substrate - A Study of Residual Stresses and Deposition Kinetics," Ph.D. Thesis, Rensselaer Polytechnic Institute, Troy, N.Y., 1974.
2. D. R. Behrendt, "Residual Stresses in Boron/Tungsten and Boron/Carbon Fibers," NASA TM X-73616, 1977.
3. R. M. Witucki, "High Modulus, High Strength Filament and Composites," Technical Report AFML-TR-66-187, Air Force Materials Laboratory, Dayton, OH, 1967.
4. J. W. Eason, "Investigation of Elongation of Boron Filament During Fabrication and Annealing," Ph.D. Thesis, University of Virginia, Charlottesville, VA, 1979.
5. T. H. Lin, Theory of Inelastic Structures, John Wiley and Sons, Inc., New York, N.Y., 1968.

TABLE I. - MATERIAL CONSTANTS

Material	Young's modulus		Poisson's ratio
	GPa	psi	
Carbon core	41.4	6×10^6	0.25
Boron sheath	39.3	57×10^6	0.13

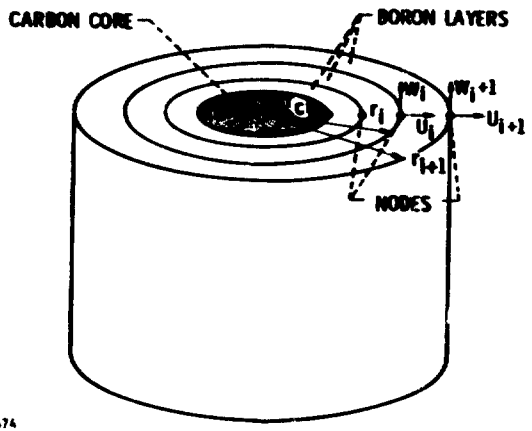

Figure 1. - Finite element of B/C filament.

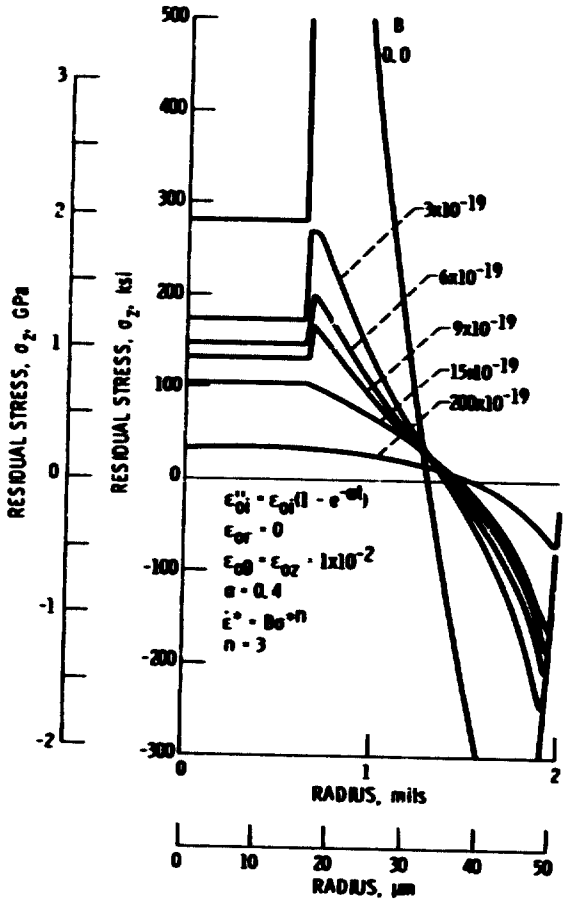

Figure 2. - Calculated axial residual stress, σ_z, versus radial location, r, as a function of B (Eq. (2)).

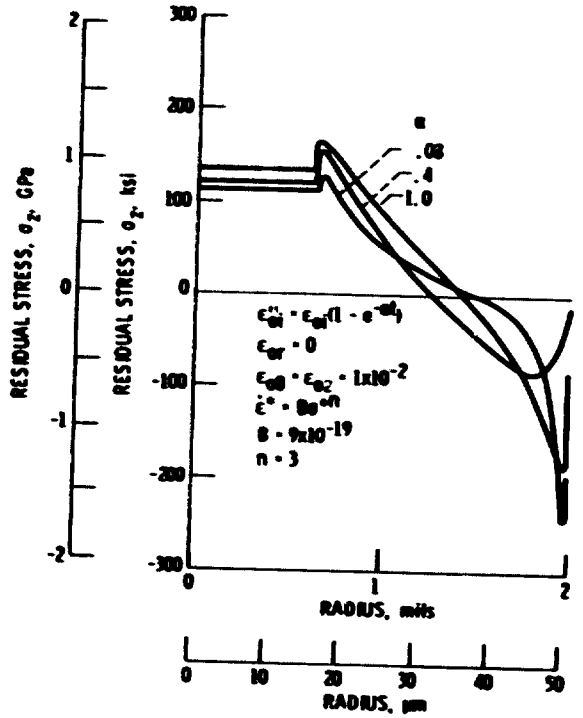

Figure 3. - Calculated axial residual stress, σ_z, versus radial location, r, as a function of α (Eq. (1)).

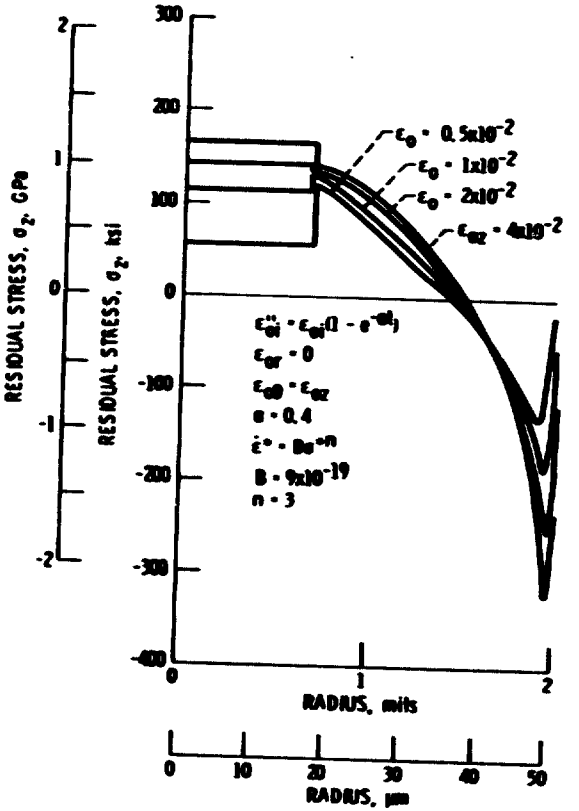

Figure 4. - Calculated axial residual stress, σ_z, versus radial location, r, as a function of $\varepsilon_{\alpha\theta}$ and $\varepsilon_{\theta z}$ (Eq. (1)).

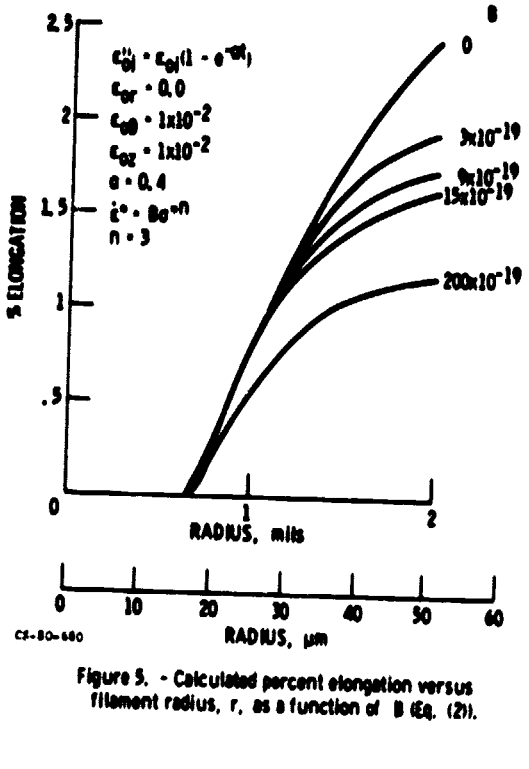

Figure 5. - Calculated percent elongation versus filament radius, r, as a function of B (Eq. (2)).

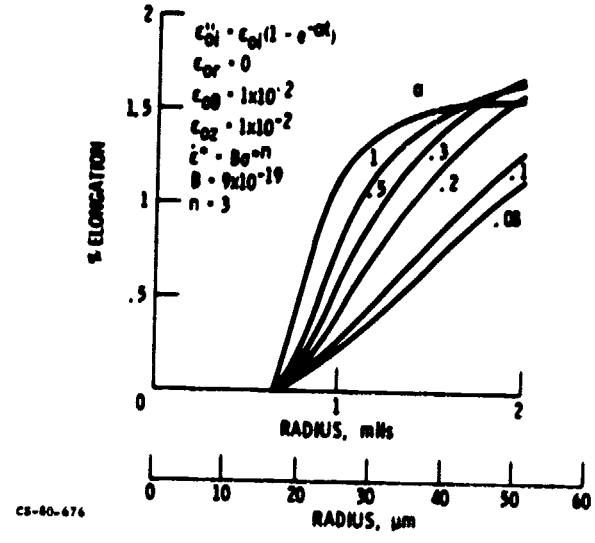

Figure 6. - Calculated percent elongation versus filament radius, r, as a function of a (Eq. (1)).

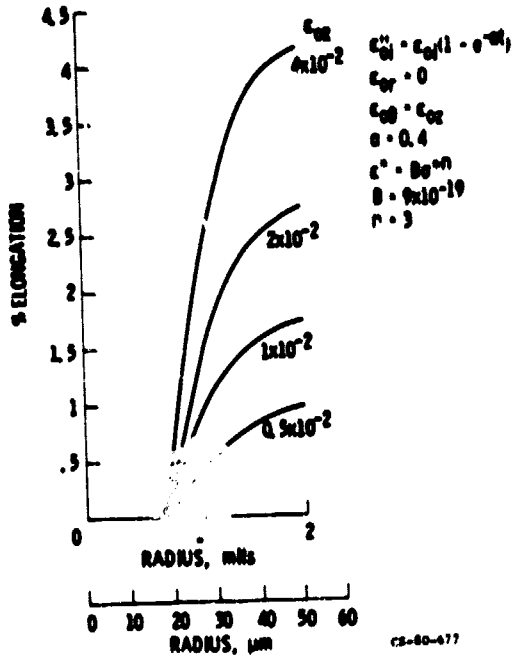

Figure 7. - Calculated percent elongation versus filament radius, r, as a function of $\varepsilon_{o\theta}$ and ε_{oz} (Eq. (1)).

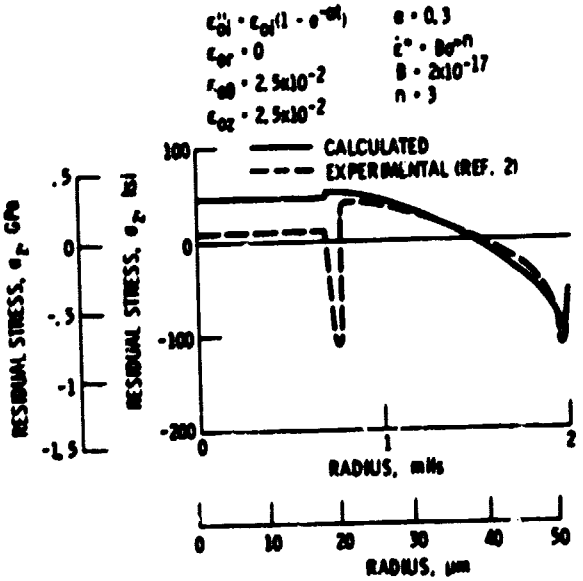

Figure 8. - Comparison of calculated and experimental axial residual stress, σ_z, versus radial location, r.

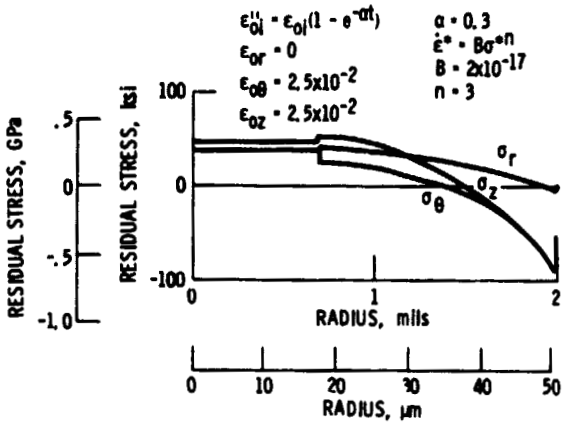

Figure 9. - Calculated residual stresses, σ_r, σ_θ, and σ_z versus radial location, r. The deposition and creep parameters are the same as that for the calculated curve in Figure 8.

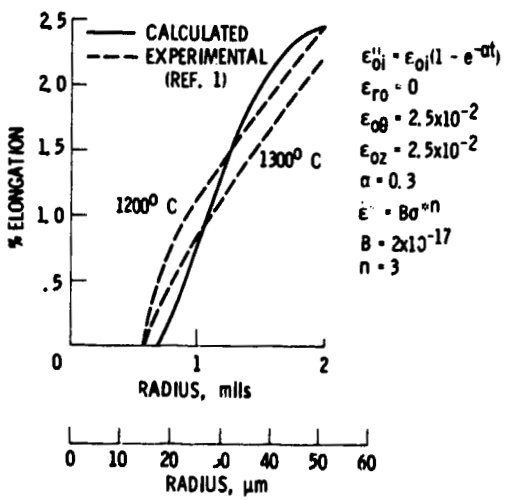

CS-80-678

Figure 10. - Comparison of the calculated and experimental elongation versus filament radius, r. The deposition and creep parameters are the same as that for the calculated curves in Figures 8 and 9.